J. Fluid Mech. (1984), *vol.* 143, *pp.* 23–46
Printed in Great Britain

Turbulent boundary-layer interaction with a shock wave at a compression corner

By S. AGRAWAL AND A. F. MESSITER
Department of Aerospace Engineering, The University of Michigan, Ann Arbor, Michigan 48109

(Received 29 July 1983)

The local interaction of an oblique shock wave with an unseparated turbulent boundary layer at a shallow two-dimensional compression corner is described by asymptotic expansions for small values of the non-dimensional friction velocity and the flow turning angle. It is assumed that the velocity-defect law and the law of the wall, adapted for compressible flow, provide an asymptotic representation of the mean velocity profile in the undisturbed boundary layer. Analytical solutions for the local mean-velocity and pressure distributions are derived in supersonic, hypersonic and transonic small-disturbance limits, with additional intermediate limits required at distances from the corner that are small in comparison with the boundary-layer thickness. The solutions describe small perturbations in an inviscid rotational flow, and show good agreement with available experimental data in most cases where effects of separation can be neglected. Calculation of the wall shear stress requires solution of the boundary-layer momentum equation in a sublayer which plays the role of a new thinner boundary layer but which is still much thicker than the wall layer. An analytical solution is derived with a mixing-length approximation, and is in qualitative agreement with one set of measured values.

1. Introduction

When a turbulent boundary layer at supersonic speed encounters a two-dimensional compression corner, details of the local mean flow are determined by an interaction between the boundary layer and an oblique shock wave. If the corner angle is not too large, at most a very small region of mean reversed flow is present. It is observed experimentally, for small turning angles, that the shock wave forms at a distance from the corner which is small in comparison with the boundary-layer thickness, and the initial rise in surface pressure is very steep. Within the boundary layer the shock wave is curved, because of the gradient in Mach number, and continuous reflections occur because of the mean vorticity. Reflected disturbances reaching the surface typically lead to a more gradual pressure increase, which continues for a distance of perhaps a few boundary-layer thicknesses, depending on the external-flow Mach number. At lower Mach numbers a pressure overshoot has been observed very close to the corner, followed by a gradual decrease toward the inviscid-flow value (Roshko & Thomke 1969).

In the flow just downstream of the corner the mean pressure gradient and acceleration are much larger, in magnitude, than in the undisturbed boundary layer. It has therefore been suggested (e.g. Roshko & Thomke 1969; Elfstrom 1972) that, if effects of separation are negligible, the mean flow changes in the boundary layer might be described approximately by inviscid-flow equations, except in regions very close to the corner and very close to the surface downstream of the corner. The

accuracy of this approximation has been confirmed by numerical calculation of surface pressures by the method of characteristics (Roshko & Thomke 1969; Rosen, Roshko & Pavish 1981). In particular cases these results show close agreement with measured values for the gradual part of the pressure increase. The calculations require that a starting value for the Mach number be supplied in some way, and there is no satisfactory method for predicting the steeper part of the pressure rise.

The inviscid-flow approximation has been developed as an asymptotic approximation for the related problem of the interaction at transonic speeds between an unseparated turbulent boundary layer and a normal shock wave, by Melnik & Grossman (1974), Adamson & Feo (1975) and Messiter (1980). A review of the important ideas, as applied to this and other problems, has been given by Melnik (1981). The velocity-defect law and the law of the wall, suitably modified for compressible flow, are assumed to provide an asymptotic description of the undisturbed, fully developed, constant-pressure turbulent boundary layer. Near the shock wave the changes in Reynolds stresses are of sufficiently high order in most of the boundary layer that the largest terms in the pressure can be calculated by solution of equations for inviscid rotational flow. Changes in the boundary-layer Reynolds stress becomes important in a sublayer which is still much thicker than the viscous wall layer (Melnik & Grossman 1974; Adamson & Feo 1975; Adamson & Liou 1980). A boundary-layer momentum equation, with a linear inertia term, is to be solved in the sublayer, for a pressure distribution which is obtained from the 'outer' inviscid-flow solution. The incompressible flow over a shallow two-dimensional bump has been studied in a similar way (Sykes 1980). These turbulent interactions are quite different from typical laminar interactions, for which the local pressure distribution is related to the change in sublayer displacement thickness, and is therefore obtained by solution of the sublayer momentum equation subject to an appropriate pressure-displacement condition. The differences arise because of the difference in form of the undisturbed velocity profiles for laminar and turbulent boundary layers.

The present investigation was motivated largely by the work of Roshko & Thomke (1969). The purposes are to obtain analytical solutions for the portion of the pressure rise which they had calculated numerically, to explore in a systematic way the implications of an asymptotic inviscid-flow description at smaller distances from the corner, and to attempt a prediction of the surface shear stress, all for unseparated flow. Details have been given by Agrawal (1983), and are summarized here. The analytical solutions for the pressure are obtained by use of supersonic, hypersonic and transonic small-disturbance approximations. Each of these solutions is found by taking an 'outer' limit of the equations, with the undisturbed boundary-layer thickness as the reference length in the direction normal to the surface. For points closer to the corner, it is necessary to study certain 'intermediate' limits, by a change of variables in the manner described by Bush (1971) for a model equation. A similar procedure has been outlined previously for the interaction at transonic speeds with a weak incident oblique shock wave (Adamson 1976) or with a weak normal shock wave (Messiter 1980, Appendix A). It is noted briefly that the presence of small-scale separation may imply a lower limit to the small lengthscales for which the intermediate solutions can properly be used. Finally, an approximate solution of a sublayer momentum equation is obtained, giving an approximate prediction of the surface shear stress.

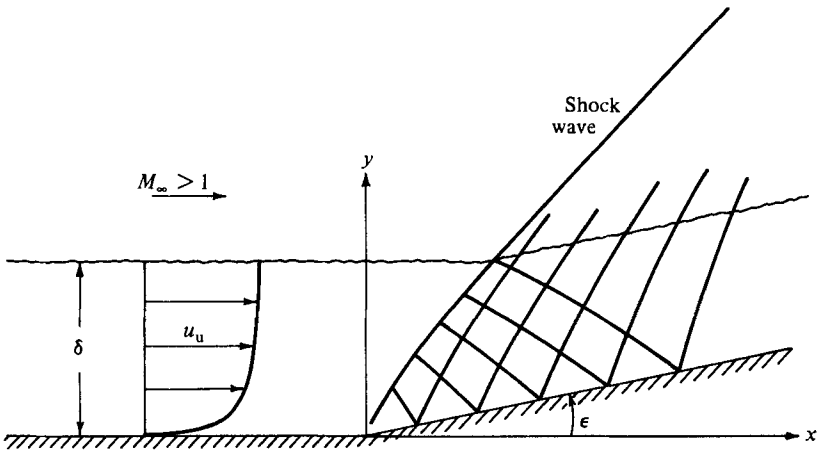

FIGURE 1. Sketch showing mean-velocity profile, shock wave and reflected waves.

2. Problem formulation

A sketch of the mean flow field is shown in figure 1. A fully developed turbulent boundary layer, at supersonic speed and high Reynolds number, encounters a shallow compression corner, giving rise to a curved shock wave which is reflected continuously as it passes through the boundary layer. Coordinates x and y, measured along and normal to the undisturbed-flow direction, have been made nondimensional with the boundary-layer thickness δ just ahead of the corner. Non-dimensional mean-velocity components u and v, in the x- and y-directions respectively, are referred to the undisturbed external-flow velocity, as are the local sound speed a and its critical value a^*. The mean values of pressure p, density ρ, temperature T and viscosity coefficient μ have been non-dimensionalized with the corresponding values in the undisturbed flow, where the Mach number is M_∞. A parameter B_∞ is defined by $B_\infty^2 = M_\infty^2 - 1$. The other two important parameters are the corner angle ϵ and the non-dimensional friction velocity $u_\tau = (\frac{1}{2}c_f)^{\frac{1}{2}}$, where c_f is the skin-friction coefficient just ahead of the corner. Throughout the following derivations it will be assumed that both ϵ and u_τ are small. Asymptotic expansions are therefore sought for $u_\tau \to 0$ and $\epsilon \to 0$.

The continuity and momentum equations are

$$\frac{\partial(\rho u)}{\partial x} + \frac{\partial(\rho v)}{\partial y} + \ldots = 0, \tag{2.1}$$

$$\rho u \frac{\partial u}{\partial x} + \rho v \frac{\partial u}{\partial y} + \frac{1}{\gamma M_\infty^2} \frac{\partial p}{\partial x} = -\frac{\partial}{\partial y}(\rho \langle u'v' \rangle) + \ldots, \tag{2.2}$$

$$\rho u \frac{\partial v}{\partial x} + \rho v \frac{\partial v}{\partial y} + \frac{1}{\gamma M_\infty^2} \frac{\partial p}{\partial y} = \ldots, \tag{2.3}$$

where the primes denote fluctuating quantities and the bracket indicates an average. Only the terms that will be needed below have been shown. The wall is taken to be insulated and the total enthalpy is approximated as being uniform. A perfect gas with constant specific heats having ratio γ is assumed. The energy equation and equation of state are

$$T = T_w - \tfrac{1}{2}(\gamma - 1) M_\infty^2 (u^2 + v^2), \quad p = \rho T + \ldots, \tag{2.4}$$

where the subscript w denotes the wall value. It may also be convenient, especially for a transonic approximation, to combine the differential equations in the form

$$(u^2-a^2)\frac{\partial u}{\partial x}+uv\left(\frac{\partial u}{\partial y}+\frac{\partial v}{\partial x}\right)+(v^2-a^2)\frac{\partial v}{\partial y}+\ldots=0. \tag{2.5}$$

The flow tangency condition at the ramp surface for $x>0$ is

$$v(x, x\tan\epsilon)=u(x, x\tan\epsilon)\tan\epsilon. \tag{2.6}$$

The shock-polar equation and the pressure jump across the shock wave are

$$v_s^2=(u_u-u_s)^2\frac{u_u u_s-a^{*2}}{\frac{2}{\gamma+1}u_u^2-u_u u_s+a^{*2}}, \tag{2.7}$$

$$p_s-p_u=\gamma M_\infty^2\rho_u u_u(u_u-u_s), \tag{2.8}$$

where the subscripts u and s refer to quantities just upstream and downstream of the shock wave. The shock-wave shape and the requirements that mass flow and tangential velocity be continuous are expressed in the form

$$S(x,y)=0, \quad [\rho\boldsymbol{q}\cdot\nabla S]=0, \quad [\boldsymbol{q}\times\nabla S]=0, \tag{2.9a, b, c}$$

where $\boldsymbol{q}$ is the non-dimensional velocity vector and the square bracket denotes a jump.

The undisturbed boundary layer for $y=O(1)$ is described by the velocity-defect law

$$u=1+u_\tau u_{01}(y), \tag{2.10}$$

where $u_{01}(y)$ has a logarithmic form as $y\to 0$, In later calculations $u_{01}(y)$ is approximated by Coles' form

$$u_{01}(y)=\kappa^{-1}\{\ln y-\Pi(1+\cos\pi y)\} \tag{2.11}$$

for $y\leqslant 1$, where $\kappa\approx 0.41$ is the von Kármán constant and Π is Coles' profile parameter; $\Pi\approx 0.5$ for a flat-plate boundary layer. For very small y, the velocity profile is expressed by the law of the wall, in terms of a coordinate $y\delta/\delta^+$, where

$$\frac{\delta^+}{\delta}=\frac{\mu_w T_w^{\frac{1}{2}}}{u_\tau Re_\delta} \tag{2.12}$$

and Re_δ is the Reynolds number based on δ and on quantities in the undisturbed external flow. That is, $y\delta/\delta^+$ is a coordinate made non-dimensional with a viscous length based on the friction velocity and the kinematic viscosity calculated using wall values ρ_w, μ_w. Expansion of the wall-layer solution for large $y\delta/\delta^+$ gives

$$u\sim u_\tau T_w^{\frac{1}{2}}\left\{\frac{1}{\kappa}\ln\left(\frac{\delta}{\delta^+ y}\right)+c\right\}, \tag{2.13}$$

where $c\approx 5.0$ as for incompressible flow, and $u_\tau T_w^{\frac{1}{2}}$ is a non-dimensional friction velocity defined in terms of the density at the wall.

A simple approximate boundary-layer profile is obtained (van Driest 1951) by use of the Prandtl mixing-length approximation

$$\tau=\rho\left(\kappa y\frac{\partial u}{\partial y}\right)^2 \tag{2.14}$$

for $\delta^+/\delta \ll y \ll 1$, where $\tau = -\rho\langle u'v'\rangle$. Since $\partial\tau/\partial y \sim 0$ and therefore $\tau \sim \tau_w = u_\tau^2$ in this range, (2.14) is easily integrated. A modified form (Maise & McDonald 1968) which remains correct for $y = O(1)$ is

$$u = \Gamma \sin\left\{\sin^{-1}\frac{1}{\Gamma} + u_\tau T_w^{\frac{1}{2}}\frac{1}{\Gamma}u_{01}(y)\right\}, \tag{2.15}$$

where $\Gamma = \{T_w/(T_w-1)\}^{\frac{1}{2}}$. Equation (2.15) is often interpreted as providing a correlation between profiles for incompressible and compressible flow. For $y = O(1)$, expansion of (2.15) for $u_\tau \ll 1$ gives the velocity-defect law (2.10). The solution (2.15) should also agree with the expansion (2.13) of the wall-layer solution when $y\delta/\delta^+$ is large but the velocity is still small, i.e. for $y\delta/\delta^+ \gg 1$ but $u_\tau \ln(y\delta/\delta^+) \ll 1$. This condition gives a relationship between u_τ and δ/δ^+ (or Re_δ):

$$u_\tau T_w^{\frac{1}{2}}\frac{1}{\kappa}\ln\frac{\delta}{\delta^+} = \Gamma\sin^{-1}\frac{1}{\Gamma} - u_\tau T_w^{\frac{1}{2}}\left(\frac{2\Pi}{\kappa}+c\right). \tag{2.16}$$

3. Outer solutions

3.1. *Supersonic limit*

The simplest description of the local pressure changes, which provides a foundation for later refinements, is obtained in a supersonic small-disturbance limit, for $\epsilon \to 0$ with M_∞ fixed. This limit leads to a straightforward linearization, since the shock wave is weak and, in a first approximation, has slope $\mathrm{d}x/\mathrm{d}y = B_\infty$, which is the same as the slopes of the outgoing characteristics. The solutions are derived in terms of coordinates x and y, and can be regarded as outer solutions; other solutions will be needed for small values of x and y.

For small u_τ the pressure is expanded in the form

$$p - 1 = p_1(\epsilon, M_\infty) + u_\tau p_2(x, y; \epsilon, M_\infty) + \ldots, \tag{3.1}$$

where p_1 is the pressure in the absence of the boundary layer and $u_\tau p_2$ represents the largest effect of the boundary layer. For small ϵ, p_1 and p_2 are expanded as

$$p_1 = \epsilon p_{11} + \epsilon^2 p_{12} + \ldots, \quad p_2 = \epsilon p_{21} + \ldots, \tag{3.2}$$

where $p_{11}, p_{12}, \ldots$ are functions of M_∞, and $p_{21}, \ldots$ depend on x, y as well. The constant terms have the known inviscid-flow values:

$$p_{11} = \frac{\gamma M_\infty^2}{B_\infty}, \quad p_{12} = \frac{\gamma M_\infty^2}{B_\infty^2}\left(-1 + \frac{\gamma+1}{4}\frac{M_\infty^4}{B_\infty^2}\right). \tag{3.3}$$

Expansions of the same form as (3.1) and (3.2), with the same subscript notation, can be written for $u - u_u$, v and $\rho - \rho_u$. It is convenient to write u_u and ρ_u in terms of a new coordinate y_u which is constant along a mean streamline and equals y at the shock wave. That is, $\rho u\,\mathrm{d}y = \rho_u(y_u)\,u_u(y_u)\,\mathrm{d}y_u$ and

$$y_u = y - \epsilon(x - B_\infty y) + \ldots, \tag{3.4}$$

$$u_u(y_u) = 1 + u_\tau u_{01}(y_u), \tag{3.5}$$

$$\rho_u(y_u) = 1 + (\gamma-1)M_\infty^2 u_\tau u_{01}(y_u) + \ldots. \tag{3.6}$$

It can be verified subsequently, as the solutions are being constructed, that the orders of magnitude shown in the expansions (3.1) and (3.2) are in fact the orders required for satisfying the differential equations and boundary conditions at each step.

Assumed forms of expansion are written in advance for conciseness only, both here and in the following sections.

The largest of the variable terms, the terms of order ϵu_τ, are easily shown to satisfy inviscid-flow equations. In the differential equations (2.1)–(2.3), which are written in terms of coordinates made non-dimensional with the boundary-layer thickness, the largest terms are $O(\epsilon u_\tau)$. For example, since the variable terms in the mean-flow quantities are $O(\epsilon u_\tau)$, $\partial u/\partial x = O(\epsilon u_\tau)$. Since the largest term in $\langle u'v' \rangle$ is of the same order as the wall shear stress, also $\partial \rho \langle u'v' \rangle / \partial y = O(u_\tau^2)$, and the perturbation in this term is still smaller. By similar arguments, it is found that all terms omitted in (2.1)–(2.3) are of higher order than ϵu_τ. It follows that in a first approximation the differential equations are the linearized inviscid-flow equations, with a vorticity perturbation in a form originally given by Sears (1950).

The solutions for u_{21} and v_{21} can be written in the form

$$u_{21} = \frac{1}{B_\infty}[1 + (\gamma - 1) M_\infty^2] u_{01}(y_u) + \phi_x(x, y), \tag{3.7}$$

$$v_{21} = u_{01}(y_u) + \phi_y(x, y), \tag{3.8}$$

$$p_{21} = -\gamma M_\infty^2 \phi_x(x, y), \tag{3.9}$$

where ϕ is a perturbation potential which satisfies the wave equation

$$B_\infty^2 \phi_{xx} - \phi_{yy} = 0. \tag{3.10}$$

It is assumed here, subject to later verification, that the term $\epsilon u_\tau v_{21}$ should be required to satisfy the tangency condition as $y \to 0$. One boundary condition, then, is given at the surface, and the other is obtained from expansion of the shock-polar equation (2.7):

$$\phi_y(x, 0) = 0, \tag{3.11}$$

$$[\phi_y + B_\infty \phi_x]_{x - B_\infty y} = \frac{2 - M_\infty^2}{B_\infty^2}\left(1 + \frac{\gamma - 1}{2} M_\infty^2\right) u_{01}(y). \tag{3.12}$$

The solution for p_{21} is easily found as

$$\frac{p_{21}}{\gamma M_\infty^2} = \frac{M_\infty^2 - 2}{2B_\infty^3}\left(1 + \frac{\gamma - 1}{2} M_\infty^2\right)\left\{u_{01}\left(\frac{x}{2B_\infty} - \frac{y}{2}\right) + u_{01}\left(\frac{x}{2B_\infty} + \frac{y}{2}\right)\right\}. \tag{3.13}$$

There are of course two contributions to p_{21} at every point, associated with reflection of the shock wave at distances $\frac{1}{2}(B_\infty^{-1} x \pm y) + \ldots$ from the surface. One disturbance arrives at (x, y) along an incoming characteristic, the other along an outgoing characteristic after reflection from the surface. If $M_\infty > \sqrt{2}$, the linear theory predicts that the reflected waves are compressions, whereas for $M_\infty < \sqrt{2}$ these waves would be expansions. At the approximate shock-wave location $x = B_\infty y$ the solution fails because the first term is logarithmically infinite. This difficulty is easily removed if B_∞ is replaced by a second approximation to the slope of the characteristics, with the shock-wave location likewise expressed by a second approximation.

The assumption of a weak shock wave can be a significant source of error in the predicted pressure distributions at values of the parameters for which experimental data are available. This error is corrected below by means of a combined supersonic–hypersonic approximation.

3.2. *Hypersonic limit*

For high Mach numbers the flow can be studied in a hypersonic small-disturbance limit, defined by $\epsilon \to 0$ and $M_\infty \to \infty$ with the hypersonic similarity parameter

$$H = \frac{1}{M_\infty^2 \epsilon^2} \tag{3.14}$$

held fixed. The shock wave is now inclined at a shallow angle $O(\epsilon)$ and is no longer weak. Disturbances in the flow behind the shock wave will overtake and be reflected from the shock, giving additional contributions to the surface pressure. The vorticity, however, is small enough that reflections of small disturbances within the boundary-layer region between the shock wave and the wall are found to be of higher order. It is assumed further that the relative change in Mach number, as well as in velocity, is small across the defect portion of the undisturbed boundary layer. Since the local Mach number M is found from $M^2/M_\infty^2 = (u^2+v^2)/T$, the change in M/M_∞ is $O(M_\infty^2 u_\tau)$. It is therefore specified that $M_\infty^2 u_\tau \to 0$ and, since $M_\infty \epsilon$ is held fixed in the hypersonic limit, that also $u_\tau/\epsilon^2 \to 0$ in this limit.

The shock-wave relations (2.7)–(2.9) can be rewritten in the form

$$S(x,y) = 0 = y - y_s(x), \tag{3.15}$$

$$y_s'^2(u_u^2 - u_u v_s y_s' - a^{*2}) = -\frac{\gamma-1}{\gamma+1}u_u^2 + u_u v_s y_s' + a^{*2}, \tag{3.16}$$

$$p_s - 1 = \gamma M_\infty^2 \rho_u u_u v_s y_s', \tag{3.17}$$

$$\frac{\rho_u}{\rho_s} = 1 - \frac{v_s(1+y_s'^2)}{u_u y_s'}, \tag{3.18}$$

where the relation $u_u - u_s = v_s y_s'$, from (2.9*c*), has been used to eliminate u_s. As in ordinary hypersonic small-disturbance theory, it is expected that the equations describing perturbations in v, p and ρ will have the same form as for unsteady one-dimensional flow. The perturbation in u does not appear in these equations.

Since the shock-wave slope $\mathrm{d}y_s/\mathrm{d}x$ is $O(\epsilon)$, the proper characteristic length in the flow direction is now δ/ϵ rather than δ. It is also convenient to choose a transverse coordinate measured relative to the surface. A suitable choice of variables is then

$$\tilde{x} = \epsilon x, \quad \tilde{y} = y - x\tan\epsilon. \tag{3.19}$$

The pressure is expanded in the form

$$p = \tilde{p}_1(\epsilon, M_\infty) + u_\tau \tilde{p}_2(\tilde{x}, \tilde{y}; \epsilon, M_\infty) + \dots, \tag{3.20}$$

where $\tilde{p}_1$ is the inviscid-flow pressure and $u_\tau \tilde{p}_2$ is the largest correction due to the boundary layer. Expansions of the same form can be written for v and ρ. The terms $\tilde{p}_1$ and $\tilde{p}_2$ can be expanded as

$$\tilde{p}_1 = \tilde{p}_{11}(H) + \dots, \quad \tilde{p}_2 = \frac{1}{\epsilon^2}\tilde{p}_{21}(\tilde{x}, \tilde{y}; H) + \dots. \tag{3.21}$$

Similar representations can be written for $\tilde{v}_1/\epsilon$ and $\tilde{v}_2/\epsilon$ and for $\tilde{\rho}_1$ and $\tilde{\rho}_2$. The shock-wave slope has the form

$$y_s' = \tilde{s}_1(\epsilon, M_\infty) + u_\tau \tilde{s}_2(\tilde{x}; \epsilon, M_\infty) + \dots, \tag{3.22}$$

where $\tilde{s}_1 = \epsilon \tilde{s}_{11}(H) + \dots$.

The largest terms are the familiar solutions for wedge flow:

$$\tilde{v}_{11} = 1, \quad \tilde{p}_{11} = 1+\frac{\gamma\tilde{s}_{11}}{H}, \quad \tilde{\rho}_{11} = \frac{\tilde{s}_{11}}{\tilde{s}_{11}-1}, \tag{3.23}$$

where

$$\tilde{s}_{11}^2 - \tfrac{1}{2}(\gamma+1)\,\tilde{s}_{11} - H = 0. \tag{3.24}$$

The perturbations $\tilde{p}_{21}$, $\tilde{v}_{21}$ and $\tilde{\rho}_{21}$ satisfy linear differential equations of the same form as for a one-dimensional unsteady flow:

$$\tilde{\rho}_{21\tilde{x}} + \tilde{\rho}_{11}\,\tilde{v}_{21\tilde{y}} = 0, \tag{3.25}$$

$$\tilde{v}_{21\tilde{x}} + \frac{H}{\gamma\tilde{\rho}_{11}}\tilde{p}_{21\tilde{y}} = 0, \tag{3.26}$$

$$\tilde{p}_{21\tilde{x}} - \frac{\gamma\tilde{p}_{11}}{\tilde{\rho}_{11}}\tilde{\rho}_{21\tilde{x}} = 0. \tag{3.27}$$

Expansion of the shock-wave relations gives

$$\tilde{s}_{11}\,\tilde{v}_{21s} = \left(\frac{4}{\gamma+1}\tilde{s}_{11}-1\right)\tilde{s}_{21} + 2\frac{\gamma-1}{\gamma+1}u_{01}, \tag{3.28}$$

$$\frac{H}{\gamma}\tilde{p}_{21s} = \tilde{s}_{11}\,\tilde{v}_{21s} + \tilde{s}_{21} + \frac{\gamma-1}{H}\tilde{s}_{11}\,u_{01}, \tag{3.29}$$

where $\tilde{p}_{21s}$ and $\tilde{v}_{21s}$ denote values at $\tilde{y} = (\tilde{s}_{11}-1)\,\tilde{x}$, and u_{01} is evaluated at $y_u = y = \tilde{s}_{11}\,\tilde{x}$. The tangency condition at the surface requires $\tilde{v}_{21} = 0$ at $\tilde{y} = 0$.

The differential equations can be combined to show that each of $\tilde{v}_{21}$ and $\tilde{p}_{21}$ satisfies a wave equation. If the tangency condition is satisfied, the solutions have the form

$$\tilde{v}_{21} = \tilde{f}(\tilde{x}+\tilde{B}\tilde{y}) - \tilde{f}(\tilde{x}-\tilde{B}\tilde{y}), \tag{3.30}$$

$$(\gamma\tilde{p}_{11}\tilde{B})^{-1}\,\tilde{p}_{21} = -\tilde{f}(\tilde{x}+\tilde{B}\tilde{y}) - \tilde{f}(\tilde{x}-\tilde{B}\tilde{y}), \tag{3.31}$$

where $\tilde{B}^2H = \tilde{\rho}_{11}/\tilde{p}_{11}$. Substitution into the shock-wave relations leads to a functional equation for $\tilde{f}$:

$$\tilde{N}\tilde{f}\{(1+\beta)\,\tilde{x}\} - \tilde{Q}\tilde{f}\{(1-\beta)\,\tilde{x}\} = -\frac{\gamma-1}{4H}(\tilde{N}+\tilde{Q})\,u_{01}(\tilde{s}_{11}\,\tilde{x}), \tag{3.32}$$

where

$$\tilde{N}+\tilde{Q} = \frac{2\tilde{s}_{11}}{4\tilde{s}_{11}-(\gamma+1)}, \quad \tilde{N}-\tilde{Q} = \frac{\tilde{B}H\tilde{p}_{11}}{2\tilde{s}_{11}}, \quad \beta = \tilde{B}(\tilde{s}_{11}-1). \tag{3.33}$$

Chu (1952) and Guiraud (1957) obtained equations similar to (3.32) by introducing small perturbations in surface slope for respectively supersonic flow past a thick wedge and hypersonic flow past a thin wedge. The ratio $|\tilde{Q}|/\tilde{N}$ in (3.32) is small: if $M_\infty\epsilon = 0$, $\tilde{Q}/\tilde{N} = 0$; if $M_\infty\epsilon \to \infty$, $\tilde{Q}/\tilde{N} \approx -0.14$ for $\gamma = 1.4$; if $M_\infty\epsilon = \frac{5}{4}$ and $\gamma = 1.4$, $\tilde{Q}/\tilde{N} \approx -0.04$. A solution for $|\tilde{Q}|/\tilde{N} < 1$ and $\beta < 1$ can be found as a series expansion in powers of $\tilde{Q}/\tilde{N}$ (Chu 1952; Guiraud 1957):

$$\tilde{f}(z) = -\frac{\gamma-1}{4H}\left(1+\frac{\tilde{Q}}{\tilde{N}}\right)\sum_{n=0}^{\infty}\left(\frac{\tilde{Q}}{\tilde{N}}\right)^n u_{01}\left\{\left(\frac{1-\beta}{1+\beta}\right)^n\frac{\tilde{s}_{11}}{1+\beta}z\right\}. \tag{3.34}$$

The solutions for $\tilde{p}_{21}$ and $\tilde{v}_{21}$ follow directly. Because of repeated reflections from the shock wave and from the surface, each of the terms $\tilde{f}(\tilde{x}+\tilde{B}\tilde{y})$ and $\tilde{f}(\tilde{x}-\tilde{B}\tilde{y})$ in the solutions depends on the values of u_{01} at an infinite sequence of points along the shock

wave. A good approximation, typically correct to within a few per cent, is found by retaining only the first term in $\tilde{f}$, thereby neglecting all reflections from the shock wave.

It is convenient to rewrite the solutions in a combined supersonic–hypersonic form by generalizing Van Dyke's (1954) suggestion to the somewhat more complicated present case. This can be accomplished by replacing M_∞ with B_∞ in the equations defining H, $\tilde{s}_{11}$ and $\tilde{p}_{11}$ and then proceeding in a manner appropriate for forming a uniformly valid composite solution from known inner and outer solutions. If additive composition is used for the terms independent of u_τ and multiplicative composition for terms proportional to u_τ (Van Dyke 1975), the result for the pressure is

$$p = \tilde{p}_{11} + \epsilon(p_{11} - \gamma B_\infty) + \epsilon^2\{p_{12} - \tfrac{1}{4}\gamma(\gamma+1)B_\infty^2\} + \frac{2u_\tau M_\infty^2}{\epsilon^2(\gamma-1)B_\infty^6}(M_\infty^2-2)\left(1+\frac{\gamma-1}{2}M_\infty^2\right)\tilde{p}_{21} + \ldots, \quad (3.35)$$

where p_{11} and p_{12} are defined as before, but $\tilde{p}_{11}$ and $\tilde{p}_{21}$ (as well as $\tilde{s}_{11}$, $\tilde{B}$, etc.) now are modified with M_∞ everywhere replaced by B_∞, as already noted. The required properties of the combined solution are easily verified: the supersonic and hypersonic solutions are recovered respectively for $M_\infty \epsilon \ll 1$ and for $M_\infty \gg 1$.

If M_∞ is close to one, the solution (3.35) of course does not remain correct, but must be replaced by a transonic approximation, as discussed in §3.3. It is also evident that (3.35) is not uniformly valid at small distances from the corner, where $\tilde{p}_{21}$ becomes logarithmically infinite. As $\tilde{x}/\tilde{B} \to 0$ and $\tilde{y} \to 0$ with $\tilde{B}\tilde{y}/\tilde{x}$ held fixed, substitution for $\tilde{p}_{21}$ from (3.31) and (3.34), if only one term is retained in $\tilde{f}$, gives

$$\tilde{p}_{21} = \frac{\gamma(\gamma-1)}{2\kappa H}\tilde{B}\tilde{p}_{11}\left\{\ln\tilde{y} + \tfrac{1}{2}\ln\left[\left(\frac{\tilde{B}\tilde{s}_{11}}{1+\beta}\right)^2\left(\frac{\tilde{x}^2}{\tilde{B}^2\tilde{y}^2}-1\right)\right] - 2\Pi\right\} + \ldots. \quad (3.36)$$

It is found that the surface pressure obtained from (3.35) differs considerably from experimental results, with an error which increases as x decreases, as shown for two cases in figure 2 and 3. At distances so small that $u_\tau \ln\tilde{y} = O(1)$, the mean velocity is no longer close to the external-flow value, and different expansions are needed. Modified solutions for small x and y are derived in §4, where comparisons with experiment are discussed in more detail.

3.3. *Transonic limit*

For low supersonic Mach numbers, solutions can be obtained in the transonic small-disturbance limit defined by $\epsilon \to 0$ and $M_\infty \to 1$ with $(M_\infty^2-1)/\epsilon^{\frac{2}{3}}$ held fixed. The shock wave is weak and nearly normal, inclined at an angle $O(\epsilon^{\frac{1}{3}})$ from the y-direction. The characteristics have slopes of the same order, but the numerical coefficients are different, so that characteristics intersect the shock wave within the flow region of interest. It is assumed further that the velocity change of order u_τ across the defect portion of the boundary layer is small in comparison with $M_\infty^2 - 1$. It will therefore be specified that $u_\tau/(M_\infty^2-1) \to 0$ and, since $(M_\infty^2-1)/\epsilon^{\frac{2}{3}}$ is held fixed in the transonic limit, that also $u_\tau/\epsilon^{\frac{2}{3}} \to 0$ in this limit.

The shock-wave shape is expressed in the form

$$S(x,y) = 0 = x - x_s(y). \quad (3.37)$$

The largest terms in the shock-polar equation (2.7) lead to the simpler transonic approximation

$$v_s^2 = \frac{\gamma+1}{2}(u_u - u_s)^2\left(\frac{u_u - a^*}{a^*} + \frac{u_s - a^*}{a^*}\right) + \ldots, \quad (3.38)$$

which is sufficient for the orders of magnitude to be considered here. The coordinate x^* and the similarity parameter K are defined by

$$x^* = \frac{x}{\epsilon^{\frac{1}{3}}}, \quad K = \frac{M_\infty^2 - 1}{\epsilon^{\frac{2}{3}}}. \tag{3.39}$$

The pressure is expanded in the form

$$p - 1 = p_1^*(\epsilon, M_\infty) + u_\tau p_2^*(x^*, y; \epsilon, M_\infty) + \ldots, \tag{3.40}$$

with similar expansions for $u - a^*$ and v. Then p_1^* and p_2^* are expanded as

$$p_1^* = \epsilon^{\frac{2}{3}} p_{11}^*(K) + \ldots, \quad p_2^* = p_{21}^*(x^*, y; K) + \ldots. \tag{3.41}$$

Expansions of the same form can be written for u_1^* and u_2^*, and for $v_1^*/\epsilon^{\frac{1}{3}}$ and $v_2^*/\epsilon^{\frac{1}{3}}$. The shock-wave slope is

$$x_s' = s_1^*(\epsilon, M_\infty) + u_\tau s_2^*(y; \epsilon, M_\infty) + \ldots, \tag{3.42}$$

where $s_1^* = \epsilon^{\frac{1}{3}} s_{11}^* + \ldots$.

The first terms in the solution describe an inviscid corner flow, and are found from

$$v_{11}^* = 1, \quad p_{11}^* = \gamma\left(\frac{K}{\gamma+1} - u_{11}^*\right), \quad s_{11}^* = \left(\frac{K}{\gamma+1} - u_{11}^*\right)^{-1}, \tag{3.43a}$$

$$\left(\frac{K}{\gamma+1} - u_{11}^*\right)^2 \left(\frac{K}{\gamma+1} + u_{11}^*\right) = \frac{2}{\gamma+1}. \tag{3.43b}$$

The velocity behind the shock wave is sonic if $u_{11}^* = 0$, and the maximum flow deflection occurs for $u_{11}^* = -\frac{1}{3}K/(\gamma+1)$.

It follows from the differential equations that u_{21}^* and v_{21}^* can be expressed in terms of a perturbation potential ϕ^*, where $u_{21}^* = u_{01} + \phi_{x^*}^*$ and $v_{21}^* = \phi_y^*$, and that ϕ^* satisfies a wave equation provided that $B^{*2} = (\gamma+1)\, u_{11}^* > 0$:

$$B^{*2}\phi_{x^*x^*}^* - \phi_{yy}^* = 0. \tag{3.44}$$

From the shock-polar equation,

$$v_{21s}^* = \frac{u_{01} - u_{21s}^*}{\dfrac{K}{\gamma+1} - u_{11}^*} + \frac{u_{01} + u_{21s}^*}{2\left(\dfrac{K}{\gamma+1} + u_{11}^*\right)}, \tag{3.45}$$

where u_{21}^* and v_{21}^* are evaluated at $x^* = s_{11}^* y$. The tangency condition at the surface requires $v_{21}^* = 0$ at $y = 0$. Since $p_{21x^*}^* + \gamma u_{21x^*}^* = 0$, and since $p_{21}^* + \gamma u_{21}^* = \gamma u_{01}$ at the shock wave, it is found that $p_{21}^* = -\gamma\phi_{x^*}^*$.

The solution for ϕ^* that satisfies the tangency condition has the form

$$\phi^* = f^*(x^* - B^* y) + f^*(x^* + B^* y). \tag{3.46}$$

Substitution in the condition obtained from the shock-polar equation again gives a functional equation

$$N^* f^{*\prime}\{(1+\beta^*)\, x^*\} - Q^* f^{*\prime}\{(1-\beta^*)\, x^*\} = \frac{1}{s_{11}^*} u_{01}\left(\frac{x^*}{s_{11}^*}\right), \tag{3.47}$$

where now

$$\beta^* = \frac{B^*}{s_{11}^*}, \quad N^* + Q^* = \frac{4B^* s_{11}^*}{\gamma+1}, \quad N^* - Q^* = 3u_{11}^* + \frac{K}{\gamma+1}. \tag{3.48}$$

Equation (3.47) has the same form as (3.32), and $|Q^*/N^*| < 1$, so that the solution has the same form as the solution (3.34). As $B^* \to 0$, however, $|Q^*/N^*| \to 1$, and at $B^* = 0$ the series diverges. The solution for $B^* = 0$ can be found directly from the functional equation (3.47) as $f^{*\prime}(x^*) = u_{01}\{Kx^*/(\gamma+1)\}$. It is also possible (Agrawal 1983) to form a combined supersonic–transonic expansion which reduces to (3.1) in the supersonic limit and to (3.40) in the transonic limit.

4. The flow close to the corner

4.1. *Intermediate solutions*

The outer solutions describe small perturbations from a uniform external flow, and therefore cannot be expected to describe the flow at points close to the corner where the velocity differs appreciably from the external-flow value. Since the upstream velocity is a function of $u_\tau \ln y$, the variation in u becomes important at values of y small enough that $u_\tau \ln y$ is no longer small. If also x is small, such that x and y are of the same order of magnitude, suitable coordinates are x/y and either $u_\tau \ln y$ or $u_\tau \ln x$. For calculation of surface pressures near the corner it appears slightly easier to choose $u_\tau \ln x$, as done by Messiter (1980); a factor $B_0 = (M_0^2-1)^{\frac{1}{2}}$, where M_0 is a local Mach number, is also included. Coordinates σ and λ are then defined by

$$\sigma = \frac{1}{\kappa} u_\tau \ln \frac{x}{B_0}, \quad \lambda = \frac{x}{B_0 y}, \tag{4.1}$$

where

$$B_0 = (M_0^2-1)^{\frac{1}{2}}, \quad M_0 = \frac{U_0}{a_0}, \tag{4.2}$$

and a_0 is a non-dimensional sound speed calculated from (2.4) with $a^2 = T/M_\infty^2$ and $u = U_0$. The velocity U_0 is an approximation to (2.15), found by expanding u_{01} for small y, setting $\kappa^{-1}u_\tau \ln y = \sigma - \kappa^{-1}u_\tau \ln \lambda$, and retaining only terms of order one:

$$U_0(\sigma) = \Gamma \sin\left\{\sin^{-1}\frac{1}{\Gamma} + \frac{1}{\Gamma} T_w^{\frac{1}{2}} \sigma\right\}. \tag{4.3}$$

Solutions are now sought in terms of perturbations about a flow with speed $u = U_0$. Sonic velocity corresponds to a value $\sigma = \sigma_a$ defined by setting $U_0 = a^*$. For $1 < M_0 < M_\infty$, and therefore $\sigma_a < \sigma < 0$, the pressure can be expanded in the form

$$p - 1 = P_1(\sigma;\epsilon) + u_\tau P_2(\sigma,\lambda;\epsilon) + \ldots. \tag{4.4}$$

As in the model problem considered by Bush (1971), the change of variable allows the intermediate solution to be obtained as a limit-process expansion, for σ and λ held fixed as $u_\tau \to 0$. If also $\epsilon \to 0$, the expansion of P_1 has the same form as the expansion (3.2) of p_1, and the solutions are the same as the solutions (3.3) except that now M_∞ is replaced by M_0 and B_∞ by B_0. Similarly, $u - u_u$ and v can be expanded in the form (4.4). For small ϵ, $P_2 = \epsilon P_{21} + \ldots$, with similar expansions for U_2 and V_2. The largest terms in U_1/U_0 and V_1/U_0 are found to give $U_{11}/U_0 = -1/B_0$, $V_{11}/U_0 = 1$, $U_{12}/U_0 = -P_{12}/\gamma M_0^2$, and $V_{12}/U_0 = -1/B_0$. These results are consistent with the differential equations and boundary conditions to the proper order, and of course remain correct as $\sigma \to 0$ and $U_0 \to 1$.

Substitution of the expansions for p, u and v into the differential equations (2.2),

(2.3) and (2.5) then gives a set of three linear differential equations for P_{21}, U_{21} and V_{21}:

$$\frac{1}{U_0}\left(U_{21\lambda}+\frac{1}{\kappa\lambda}U'_{11}\right)+\frac{1}{\gamma M_0^2}\left(P_{21\lambda}+\frac{1}{\kappa\lambda}P'_{11}\right)=0, \tag{4.5}$$

$$\frac{1}{U_0}\left(V_{21\lambda}+\frac{1}{\kappa\lambda}V'_{11}\right)-\frac{1}{\gamma M_0^2}\lambda B_0 P_{21\lambda}=0, \tag{4.6}$$

$$U_{21\lambda}+\frac{1}{\kappa\lambda}U'_{11}+\frac{\lambda}{B_0}V_{21\lambda}+\frac{1}{\kappa B_0}U'_0=0. \tag{4.7}$$

It is seen that σ enters only as a parameter, and so these are ordinary differential equations in λ. For any value of σ, the definition (4.1) implies that the reference length for x and y is $\Delta(\sigma)=\exp(\kappa\sigma/u_\tau)$. If $x=O(\Delta)$ and $y=O(\Delta)$, the velocity is close to $U_0(\sigma)$ and the shock wave is nearly plane. One might also note that the vorticity is $v_x-u_y=-\kappa^{-1}u_\tau/y+\ldots$, and so a similarity argument could have been used to show, for a given σ, that the flow perturbations P_{21}, U_{21}, and V_{21} depend only on the similarity variable $\lambda=x/B_0y$. If a tangency condition is assumed at the surface, again subject to later verification, then as $\lambda\to\infty$

$$V_{21}\sim-\frac{1}{\kappa}(\ln\lambda+2\Pi)\,U'_0. \tag{4.8}$$

The shock-wave relations give

$$\frac{V_{21}}{U_0}+B_0\frac{U_{21}}{U_0}=-\frac{M_0^2U'_0}{\kappa B_0^2U_0}\left(1+\frac{\gamma-1}{2}M_0^2\right)(\ln\lambda_s+2\Pi), \tag{4.9}$$

$$\frac{1}{\gamma M_0^2}P_{21}+\frac{1}{U_0}U_{21}=-\frac{U'_0}{\kappa B_0U_0}\{1+(\gamma-1)M_0^2\}(\ln\lambda_s+2\Pi), \tag{4.10}$$

where $\lambda_s=1+O(\epsilon)$. Solution of the system (4.5)–(4.10) gives, eventually,

$$\frac{1}{\gamma M_0^2}P_{21}=\frac{U'_0}{\kappa B_0^3U_0}\left(1+\frac{\gamma-1}{2}M_0^2\right)(M_0^2-2)\left(\tfrac{1}{2}\ln\frac{\lambda^2-1}{4}-\ln\lambda-2\Pi\right). \tag{4.11}$$

The range of validity of these intermediate solutions can be extended by some rather simple modifications. If $\kappa^{-1}\{\ln(x\pm B_0y)-\ln 2B_0-2\Pi\}$ is replaced by $u_{01}\{(x\pm B_0y)/2B_0\}$, the term (4.11) remains correct when $y=O(1)$. That is, the modified expression contains both the outer and the intermediate solutions. Next, hypersonic as well as supersonic limits can be included if the derivations of this section are repeated for hypersonic intermediate limits such that $M_0\epsilon=O(1)$. A single expression for the pressure can then be written for all M_0 such that $M_0^2-1\gg\epsilon^{\frac{2}{3}}$ and $M_0^2u_\tau\ll1$. The result, obtained using the procedure already described, is

$$p=\tilde{P}_{11}+\epsilon(P_{11}-\gamma B_0)+\epsilon^2\{P_{12}-\tfrac{1}{4}\gamma(\gamma+1)B_0^2\}+\ldots$$
$$+\frac{M_0^2U'_0}{B_0^4U_0}(M_0^2-2)\left(1+\frac{\gamma-1}{2}M_0^2\right)\left\{-\gamma\tilde{B}_0\tilde{P}_{11}\sigma+\frac{2u_\tau\tilde{P}_{21}}{(\gamma-1)\epsilon^2B_0^2}\right\}+\ldots, \tag{4.12}$$

where $B_0^2=M_0^2-1$ and

$$P_{11}=\frac{\gamma M_0^2}{B_0},\quad P_{12}=\frac{\gamma M_0^2}{B_0^2}\left(\frac{\gamma+1}{4}\frac{M_0^4}{B_0^2}-1\right), \tag{4.13}$$

$$\tilde{P}_{11}=1+\gamma B_0^2\epsilon^2\tilde{S}_{11},\quad 0=\tilde{S}_{11}^2-\frac{\gamma+1}{2}\tilde{S}_{11}-\frac{1}{B_0^2\epsilon^2}, \tag{4.14}$$

$$\tilde{P}_{21} = -\gamma \tilde{B}_0 \tilde{P}_{11} \{\tilde{f}_0(\tilde{x} + \tilde{B}_0 \tilde{y}) + \tilde{f}_0(\tilde{x} - \tilde{B}_0 \tilde{y})\}, \tag{4.15}$$

$$\tilde{f}_0(z) = -\tfrac{1}{4}(\gamma - 1) B_0^2 \epsilon^2 \left(1 + \frac{Q}{N}\right) \sum_{n=0}^{\infty} \left(\frac{Q}{N}\right)^n u_{01} \left\{\left(\frac{1-\beta_0}{1+\beta_0}\right)^n \frac{\tilde{S}_{11}}{1+\beta_0} z\right\}, \tag{4.16}$$

$$\beta_0 = \tilde{B}_0(\tilde{S}_{11} - 1), \quad \tilde{B}_0^2 \tilde{P}_{11} = \frac{B_0^2 \epsilon^2 \tilde{S}_{11}}{\tilde{S}_{11} - 1}, \tag{4.17}$$

$$N + Q = \frac{2\tilde{S}_{11}}{4\tilde{S}_{11} - (\gamma + 1)}, \quad N - Q = \frac{\tilde{B}_0 \tilde{P}_{11}}{2B_0^2 \epsilon^2 \tilde{S}_{11}}. \tag{4.18}$$

Equation (4.12) is a composite solution which remains correct in the outer and intermediate supersonic and hypersonic limits defined above. For numerical calculations, u_{01} can be approximated by (2.11). When $x > B_\infty$, values $M_0 > M_\infty$ can be avoided by setting $\sigma = 0$; the effect is to replace (4.12) with the outer solution (3.35).

4.2. *Comparisons with experiment*

Numerical results for the surface pressure have been calculated for some of the cases studied by Roshko & Thomke (1969). The pressure obtained from (4.12) is plotted in figure 2 for $M_\infty = 4.92$, $\epsilon \approx 15°$, and $u_\tau = 0.017$, and in figure 3 for $M_\infty = 3.93$, $\epsilon \approx 15°$, and $u_\tau = 0.018$. The agreement with the experimental data is seen to be very good, with a typical error in pressure of less than 2 % for $M_\infty \approx 5$ and perhaps 3 % for $M_\infty \approx 4$. Roshko & Thomke (1969) and Rosen *et al.* (1981) have also shown numerical solutions obtained by the method of characteristics for $M_\infty = 3.93$. Since the numerical solutions are almost coincident with the data, the theoretical and numerical solutions are likewise in very close agreement. The combined supersonic–hypersonic outer solution (3.35), indicated by dashed lines in figures 2 and 3, is seen to be accurate near the end of the pressure rise, but shows an increasing error as x decreases, and so is clearly not satisfactory. The solutions (3.35) and (4.12) approach the inviscid-flow value in an oscillatory manner, with maximum overshoot of roughly 2 % of the overall pressure rise in figure 2 or figure 3, at larger values of x than are shown in the figures. This effect is associated with the sign change which occurs when a weak pressure disturbance overtakes and is reflected from the shock wave, and is very small because the reflected disturbances are considerably weaker than the incident disturbances, as can be seen from (3.34) since $|\tilde{Q}|/N$ is small. The experimental data show a larger overshoot of perhaps between 4 and 8 %, and the theoretical solution thus does not completely account for this effect. It seems possible that a small error would arise because the neglected decrease in Mach number with decreasing y would tend to amplify the small pressure overshoot. The needed correction might then appear in higher-order terms of the expansions, but it is not clear that this is the only important omitted contribution to the overshoot.

Thus the relatively simple analytical result (4.12) successfully duplicates results obtained by numerical integration, and now no assumption is needed about a proper starting point for the calculation. The numerical solution of Roshko & Thomke (1969), on the other hand, required introduction of an empirically determined slip Mach number. Similarly, Rosen *et al.* (1981) carried out a characteristics calculation with the starting value obtained by use of an integral method. The present results, however, still do not include a prediction of the observed very steep initial part of the pressure rise.

Equation (4.12) can be shown to predict a minimum in the surface pressure, at a value of M_0 which depends on the parameters and which corresponds to a location too close to the corner to be shown conveniently in figures 2 and 3. For still smaller

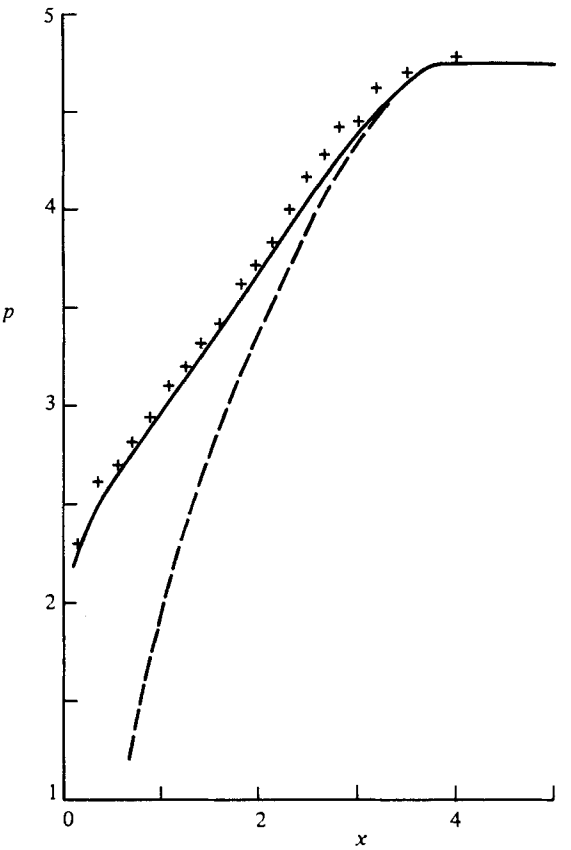

FIGURE 2. Wall pressure for $M_\infty = 4.92$, $\epsilon = 14.86°$, $u_\tau = 0.01658$: ——, calculated from (4.12); – – –, calculated from (3.35); +, experimental data (Roshko & Thomke 1969).

values of M_0, (4.12) clearly is no longer correct, and must be replaced by a transonic approximation. If $M_0 \to 1$, and therefore $B_0 \to 0$, (4.12) gives

$$p = 1 + \frac{\gamma\epsilon}{B_0} + \frac{\gamma(\gamma+1)\,\epsilon^2}{4B_0^4} + \ldots + \frac{\gamma(\gamma+1)\,M_\infty\,\epsilon u_\tau}{2B_0^3\kappa}\left\{\ln\frac{x}{B_0} - \tfrac{1}{2}\ln\frac{x^2 - B_0^2 y^2}{4B_0^2} + 2\Pi\right\} + \ldots . \tag{4.19}$$

As in ordinary transonic small-disturbance theory, a different solution is needed when $M_0 - 1 = O(\epsilon^{\frac{2}{3}})$. Some of the details are shown in the Appendix, with the assumption that the turning angle at the shock wave remains equal to ϵ in the first approximation. This formulation permits subsonic velocity behind the shock wave, but fails when M_0 is too close to the detachment value M_d, the minimum value for which an oblique shock wave can turn the flow through an angle ϵ. If the turning angle at the shock wave remains nearly equal to ϵ at even smaller distances, it is found that still another solution is required when $M_0 - M_d = O(\epsilon^{\frac{2}{3}}\chi^{\frac{1}{3}})$, where $\chi = u_\tau/\epsilon^{\frac{2}{3}} \ll 1$. The corresponding solution is discussed briefly in the Appendix. Finally, the formulation which would describe detachment of the shock wave corresponds to a limit such that $M_0 - M_d = O(u_\tau)$, as also noted in the Appendix.

A solution describing detachment would, however, predict a maximum pressure at least as large as the pressure behind a normal shock wave at $M_0 = M_d$, whereas for $3 \lesssim M_0 \lesssim 5$ no such behaviour is observed experimentally. A different possibility

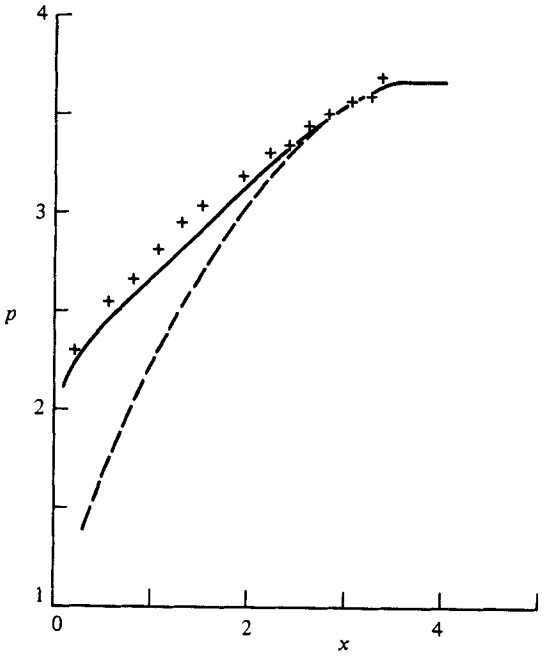

FIGURE 3. Wall pressure for $M_\infty = 3.93$, $\epsilon = 15.06°$, $u_\tau = 0.01844$: ——, calculated from (4.12); – – –, calculated from (3.35); +, experimental data (Roshko & Thomke 1969).

is a shock wave which is everywhere oblique and which is formed by coalescence of compression waves arising through interaction with a sublayer, at points very close to the corner, in a manner which has not been properly recognized here. It also seems likely that fluctuations in shock-wave location and shape could have a considerable smoothing effect on the local mean surface pressure. The importance of these intermittency effects has recently been demonstrated by Dolling & Murphy (1983) for a case with separation, and somewhat smaller effects would presumably be present for the cases of figures 2 and 3. Moreover, as argued below, a very small region of reversed mean flow may have been present in each of these latter cases.

Attempts at detecting incipient separation have been made by a variety of techniques, with results which have sometimes appeared contradictory. In particular, surface-flow studies (e.g. Appels & Richards 1975) have identified regions of reversed mean flow considerably smaller than are recognized by most other methods. Roshko and Thomke (1976) defined an interaction length l for separated flows as the distance upstream from the corner to the intersection of a tangent drawn at the inflection point of the wall-pressure curve with the x-axis, and suggested an empirical formula for l as a function of ϵ and u_τ, independent of M_∞. They noted that incipient separation detected by liquid-line observations corresponds to a value $l \approx 0.1\delta$. For example, if $u_\tau = 0.022$, as in one of the tests carried out for $\epsilon = 10°$ and $M_\infty = 2.95$, inversion of the expression for l gives $\epsilon \approx 14.5°$, somewhat larger than the actual value in the experiment,. If instead the values $\epsilon = 10°$ and $u_\tau = 0.022$ are specified, one finds $l \approx 0.01\delta$, and the region of reversed mean flow would then have length somewhat larger than 0.01δ. For comparison, according to formulas given earlier, in this case the upstream wall-layer thickness was $\delta^+ \approx 0.00004\delta$, and the distance from the wall to the sonic line was about 0.0008δ ahead of the shock wave and 0.009δ just downstream; the reference length in the flow direction is smaller than this last value

by a factor $O(\epsilon^{\frac{1}{3}})$, whereas the estimated value of l is larger. The presence of this small-scale separation therefore appears to imply that inviscid-flow solutions for M_0 near one may have to be coupled with a description of the small region of reversed mean flow.

The data of Roshko & Thomke (1969) for $M_\infty \approx 3$ have the same form as for $M_\infty \approx 4$ and 5 (figures 2 and 3), but the predicted pressure is now found to be too low by about 8% of the absolute pressure or about 13% of the pressure increase. Their measured pressure distributions for $M_\infty \approx 2.0$, however, show quite different behaviour. The pressure rises rapidly to a maximum, well above the inviscid-flow value, at a point quite close to the corner, and then shows a gradual decrease; for $\epsilon \approx 5°$ or 10°, the separation bubble again appears to remain very small. The present solution (4.12) would instead predict a pressure below the final inviscid-flow value in most of the boundary layer. The predicted trend would be reversed only at still lower Mach numbers, as a result of the factor $M_0^2 - 2$ in (4.12). The reasons for these discrepancies are not yet understood.

5. Sublayer solutions

5.1. *Formulation of sublayer problem*

In principle the asymptotic flow description can be carried further to allow calculation of changes in the wall shear stress τ_w from the upstream value $\tau_w = u_\tau^2$ (e.g. Melnik & Grossman 1974; Adamson & Liou 1980; Sykes 1980). The situation is, however, less satisfying than for the pressure calculation, because eventually an assumption regarding the form of the Reynolds stress is needed, and because fewer experimental data are available for comparison. As a first step, the problem of calculating τ_w can be partially formulated, with no choice yet made for a closure condition.

The largest terms in the 'outer' solutions given earlier are derived from inviscid-flow equations, which do not contain enough information for calculation of changes in the wall shear stress. The flow details must also be studied in a sublayer where the changes in turbulent stresses are important. This sublayer plays the role of a new, thinner boundary layer, in an inviscid rotational external flow described by the outer solutions. From a different view, the Reynolds stress in the very thin wall layer is nearly in equilibrium with the local value of the wall shear stress, and cannot be expected to match with the Reynolds stress in the outer part of the boundary layer, which depends primarily on upstream history. Instead, the perturbations in the wall-layer solution and in the outer solution are to be matched with the perturbations in the sublayer. This sublayer has been called a 'Reynolds-stress sublayer' (Adamson & Feo 1975) or a 'blending layer' (Melnik & Grossman 1974).

In the wall layer $y = O(\delta^+/\delta)$, where δ^+ is defined by (2.12), and the pressure gradient $\mathrm{d}p/\mathrm{d}x = O(\epsilon u_\tau)$, as in the outer part of the boundary layer where $y = O(1)$. Since the velocity u remains $O(u_\tau)$ and $x = O(1)$, the acceleration $uu_x = O(u_\tau^2)$. The terms representing effects of laminar and turbulent shear stresses are, however, $O(u_\tau^2 \delta/\delta^+)$, which is much larger, and so the momentum equation again expresses a balance between these two terms, with the coordinate x appearing as a parameter. Just as in the undisturbed boundary layer, the flow variables depend on local values of the wall-layer thickness and the non-dimensional friction velocity, now given respectively by $\delta^+ u_\tau/(\tau_w p_w)^{\frac{1}{2}}$ and $(\tau_w/\rho_w)^{\frac{1}{2}}$. A suitable wall-layer coordinate downstream of the corner is then

$$y^+ = \frac{\tau_w^{\frac{1}{2}} p_w^{\frac{1}{2}}}{u_\tau} \frac{(y - x\tan\epsilon)\,\delta}{\delta^+}. \tag{5.1}$$

The mean-velocity profile obtained from (2.14) for large y^+ becomes

$$u = \Gamma \sin\left\{T_{\mathrm{w}}^{\frac{1}{2}} \frac{1}{\Gamma}\left(\frac{\tau_{\mathrm{w}}}{p_{\mathrm{w}}}\right)^{\frac{1}{2}}\left(\frac{1}{\kappa}\ln y^+ + c\right)\right\}. \tag{5.2}$$

Equation (5.2) differs from the corresponding undisturbed profile only in the replacement of u_τ by $(\tau_{\mathrm{w}}/p_{\mathrm{w}})^{\frac{1}{2}}$. The dependence of the temperature and density on y^+ does not appear in the first approximation to the wall-layer momentum equation, and so the integration constant c has the same value as for a constant-density flow (e.g. Melnik & Grossman 1974).

In terms of a sublayer coordinate $\hat{y}$ the expanded wall-layer solution (5.2) becomes

$$\begin{aligned} u - 1 - u_\tau \hat{u}_{01} = {} & C_\infty\left(\frac{\tau_{\mathrm{w}}^{\frac{1}{2}}}{u_\tau p_{\mathrm{w}}^{\frac{1}{2}}} - 1\right) - \tfrac{1}{2}(T_{\mathrm{w}} - 1) C_\infty^2 \left(\frac{\tau_{\mathrm{w}}^{\frac{1}{2}}}{u_\tau p_{\mathrm{w}}^{\frac{1}{2}}} - 1\right)^2 \\ & + u_\tau (1 + C_\infty - T_{\mathrm{w}} C_\infty)\left(\frac{\tau_{\mathrm{w}}^{\frac{1}{2}}}{u_\tau p_{\mathrm{w}}^{\frac{1}{2}}} - 1\right)\hat{u}_{01} + \frac{u_\tau}{2\kappa}\ln\left(\frac{\tau_{\mathrm{w}} p_{\mathrm{w}}}{u_\tau^2}\right) + \ldots, \end{aligned} \tag{5.3}$$

where

$$\hat{u}_{01} = \frac{1}{\kappa}\left(-\ln\frac{\delta}{\hat{\delta}} + \ln\hat{y} - 2\Pi\right), \tag{5.4}$$

$$\hat{y} = (y - \epsilon x)\,\delta/\hat{\delta}, \tag{5.5}$$

$$C_\infty = \frac{\Gamma}{T_{\mathrm{w}}^{\frac{1}{2}}} \sin^{-1}\frac{1}{\Gamma}, \tag{5.6}$$

and $\hat{\delta}$ is still to be determined. The sublayer solution for u is to be derived in terms of coordinates x and $\hat{y}$. When evaluated as $\hat{y} \to 0$ this solution must agree with the solution (5.3), and the expansion as $\hat{y} \to \infty$ must match with the expansion of the outer solution as $y \to 0$.

The matching conditions and the differential equations suggest an expansion of u in the form

$$u - u_{\mathrm{u}} = \hat{u}_1(\epsilon, M_\infty) + u_\tau \hat{u}_2(x, \hat{y}; \epsilon, M_\infty, \ln(\delta/\hat{\delta})) + \ldots, \tag{5.7}$$

where now $u_{\mathrm{u}} = 1 + u_\tau \hat{u}_{01} + \ldots$ and

$$\hat{u}_1 = -\frac{\epsilon}{B_\infty} + \frac{\epsilon^2}{B_\infty^2}\left\{1 - \frac{(\gamma+1) M_\infty^4}{4B_\infty^2}\right\} + \ldots, \tag{5.8}$$

$$\hat{u}_2 = \epsilon \hat{u}_{21}(x, \hat{y}; M_\infty, \ln(\delta/\hat{\delta})) + \ldots. \tag{5.9}$$

The terms shown in (5.8) for $\hat{u}_1$ are the same as obtained in the outer solution. For conciseness the dependence on $\ln(\delta/\hat{\delta})$ is included in $\hat{u}_2$ rather than written separately. Similar expansions are found for v, $p-1$, and $\rho - \rho_{\mathrm{u}}$. The orders of magnitude appearing in the expansion of τ_{w}, and therefore also in the shear stress away from the wall, are determined from the matching of the solutions (5.3) and (5.7) for u. The shear stress is thereby found to have the form

$$\frac{\tau}{u_\tau^2} = \tau_1(x, \hat{y}; \epsilon, M_\infty) + u_\tau \tau_2(x, \hat{y}; \epsilon, M_\infty, \ln(\delta/\hat{\delta})) + \ldots \tag{5.10}$$

$$= 1 + \epsilon\tau_{11} + \epsilon^2\tau_{12} + \ldots + u_\tau \epsilon\tau_{21} + \ldots. \tag{5.11}$$

When evaluated at $\hat{y} = 0$, (5.11) becomes the expansion for τ_{w}. If the expansions for p_{w} and τ_{w} are substituted in (5.3) and the result compared with (5.7) and (5.8), the largest perturbation in τ_{w} is easily seen to be $\epsilon B_\infty^{-1}(\gamma M_\infty^2 - 2/C_\infty)$. Thus

$\tau_{11}(x,0) = B_\infty^{-1}(\gamma M_\infty^2 - 2/C_\infty)$. The term of order ϵ^2 is likewise constant and is found in the same way. These terms in τ_w can therefore be obtained without prior derivation of a new solution for the sublayer. The term of order $\epsilon u_\tau \ln(\hat{y}\hat{\delta}/\delta)$ in (5.3) is, however, different from the corresponding term in the expansion of the outer solution as $y \to 0$, and now a sublayer solution is required.

If the pressure gradient and shear stress are both to appear in the first approximation to the sublayer momentum equation, it follows that the sublayer thickness is $\hat{\delta} = O(u_\tau \delta)$; it is sufficient to set $\hat{\delta} = u_\tau \delta$. Then $\hat{p}_{21\hat{y}} = 0$ and

$$\hat{u}_{21x} = -\frac{1}{\gamma M_\infty^2}\hat{p}_{21x} + \tau_{11\hat{y}}, \tag{5.12}$$

where $\hat{p}_{21} = p_{21}(x,0)$ from matching with the outer solution. Since it can be shown from the continuity equation that $\hat{v}_{21\hat{y}} = \mathrm{d}\hat{u}_{01}/\mathrm{d}\hat{y}$, and the tangency condition requires $\hat{v}_{21} - \hat{u}_{01} \to 0$ as $\hat{y} \to 0$, it is found that $\hat{v}_{21} = \hat{u}_{01}(\hat{y})$. This term, however, does not contribute to the streamline slope v/u. The variable term in v/u is $O(\epsilon u_\tau^2)$, and the corresponding displacement effect of the sublayer does not influence the larger terms calculated in the outer solution. In particular, it follows that the tangency condition in the form (3.11) does provide a correct boundary condition.

The matching condition for u as $\hat{y} \to \infty$ suggests expressing $\hat{u}^{21}$ by

$$\hat{u}_{21} = -\frac{1}{\gamma M_\infty^2}\hat{p}_{21} + \frac{1}{B_\infty}[1 + (\gamma - 1)M_\infty^2]\hat{u}_{01} + \hat{u}(x,\hat{y}), \tag{5.13}$$

where

$$\hat{u}_x = \tau_{11\hat{y}} \tag{5.14}$$

and $\hat{u} \to 0$ as $\hat{y} \to \infty$. Also $\tau_{11}(x,0) = B_\infty^{-1}(\gamma M_\infty^2 - 2/C_\infty)$, as already noted. The outer solution with u_{01} replaced by $\hat{u}_{01}$ can be shown to remain correct when $x = O(\hat{\delta}/\delta)$ and $y = O(\hat{\delta}/\delta)$. As $x \to 0$, then, the solution for u must match with the rewritten outer solution, which in turn satisfies the proper shock-wave relations. The initial condition for $\hat{u}$ in (5.14) is therefore found to be $\hat{u} \to 0$ as $x \to 0$. Similarly, the solution $\hat{v}_{21} = \hat{u}_{01}$ matches correctly as $x \to 0$.

5.2. *Approximate calculation of wall shear stress*

It is only at this point that a representation of the changes in turbulent shear stresses is required. Only the simplest possibility, the mixing-length description (2.14), is considered here. For this choice an analytical solution can be obtained and the possibility of at least qualitative agreement with experimental results can be demonstrated with a minimum of effort.

Expansion of (2.14) gives $\tau_{11} = 2\kappa(\hat{y}\hat{u}_{21\hat{y}})$, which leads to the proper form for $\hat{u}$ as $\hat{y} \to 0$ and gives $\hat{u} \to 0$ as $\hat{y} \to \infty$. The change in τ_{11} across the sublayer influences the change in $\hat{u}_{21}$ as $\hat{y} \to 0$, which in turn affects the term τ_{21} at the wall. Since $\tau_{11} \to$ constant as $\hat{y} \to 0$, it can be seen that the differential equations and matching conditions are satisfied by a self-similar solution of the form $\hat{u} = f(\hat{y}/x)$. The result that satisfies all the proper conditions is

$$\hat{u} = \frac{1}{\kappa B_\infty}\left(1 + \frac{\gamma - 1}{2}M_\infty^2 + \frac{1}{C_\infty}\right)\int_{\hat{y}/2\kappa x}^{\infty} \frac{1}{\eta}\mathrm{e}^{-\eta}\,\mathrm{d}\eta. \tag{5.15}$$

The sublayer velocity (5.7) can now be expanded as $\hat{y} \to 0$ and compared term by term with the expansion (5.3) of the wall-layer velocity, with p_w replaced by the

solution (3.1) evaluated as $y \to 0$. After some algebra, the first few terms in τ_w are found as

$$\tau_{11w} = p_{11} - \frac{2}{B_\infty C_\infty}, \tag{5.16a}$$

$$\tau_{12w} = \frac{p_{12}}{\gamma M_\infty^2} B_\infty \tau_{11w} + \frac{1}{B_\infty^2}\left(\frac{1}{C_\infty^2} - \frac{1+3\gamma}{2C_\infty} M_\infty^2\right), \tag{5.16b}$$

$$\tau_{21w} = \frac{\hat{p}_{21}}{\gamma M_\infty^2} B_\infty \tau_{11w} + \frac{2}{\kappa B_\infty C_\infty}\left\{\frac{1}{C_\infty} - \gamma M_\infty^2 - \left(\frac{1}{C_\infty} + 1 + \frac{\gamma-1}{2} M_\infty^2\right) \times (\gamma_e + 2\Pi - \ln 2\kappa u_\tau x)\right\} + \dots, \tag{5.16c}$$

where $\gamma_e = 0.577\dots$ is the Euler constant; p_{11} and p_{12} are given by (3.3).

At least three possibilities for improvement of the solution for τ_w can easily be recognized. Modifications can be derived to allow application at smaller values of x and at higher Mach numbers, and a more detailed description of the turbulent shear stress, perhaps along the lines proposed by Melnik & Grossman (1974) or by Sykes (1980), might be attempted. Thus far only the first of these extensions has been carried out, by the use of intermediate solutions for smaller values of x.

For very small distances from the corner, the momentum equation expresses a balance of inertia, pressure and Reynolds-stress terms, as in (5.12), when $\hat{y} = O(x)$. Thus the sublayer thickness defined in this way decreases as $x \to 0$. Again with the use of the mixing-length approximation, the term proportional to ϵu_τ in u is found to depend on σ, $\hat{y}/x$ and $\ln u_\tau$. The result for u is

$$u - u_u = \epsilon U_{11} + \epsilon^2 U_{12} - u_\tau \epsilon \frac{U_0 \hat{P}_{21}}{\gamma M_0^2} - u_\tau \epsilon \frac{U_0'}{\kappa B_0}\{1 + (\gamma-1) M_0^2\} \times \left\{\ln \frac{x}{B_0 u_\tau \hat{y}} + 2\Pi\right\} + u_\tau \epsilon \frac{U_0'}{\kappa B_0}\left(1 + \frac{\gamma-1}{2} M_0^2 + \frac{U_0}{C_0 U_0'}\right) \times \int_{U_0 \hat{y}/2\kappa U_0' x}^{\infty} \eta^{-1} e^{-\eta} \, d\eta + \dots, \tag{5.17}$$

where

$$u_u = U_0(\sigma) - (u_\tau/\kappa)(\ln \lambda - 2\Pi) U_0'(\sigma) + \dots \quad \text{and} \quad C_0 = \frac{\Gamma}{T_w^{\frac{1}{2}}} \sin^{-1} \frac{U_0}{\Gamma}. \tag{5.18}$$

Also $\hat{P}_{21}$ is the value of P_{21} obtained as $\lambda \to \infty$. Equation (5.17) matches properly with the inviscid-flow intermediate solution as $\hat{y} \to \infty$ and matches with the sublayer solution (5.7) as $\sigma \to 0$.

The expansion of the wall-layer solution for large y^+ is

$$u - u_u = U_0' C_0\left(\frac{\tau_w^{\frac{1}{2}}}{u_\tau p_w^{\frac{1}{2}}} - 1\right) - \tfrac{1}{2} U_0 (T_w - 1) C_0^2 \left(\frac{\tau_w^{\frac{1}{2}}}{u_\tau p_w^{\frac{1}{2}}} - 1\right)^2 + \frac{u_\tau}{\kappa}\{U_0' - U_0 C_0 (T_w - 1)\}\left(\frac{\tau_w^{\frac{1}{2}}}{u_\tau p_w^{\frac{1}{2}}} - 1\right)\left(\ln \frac{B_0 \hat{y}}{x} - 2\Pi\right) + \frac{u_\tau}{2\kappa} U_0' \ln \frac{\tau_w p_w}{u_\tau^2} + \dots. \tag{5.19}$$

Comparison of (5.17) and (5.19) then yields an intermediate expansion for τ_w when x is small, such that $\sigma_a < \sigma < 0$, in the form

$$\frac{\tau_w}{u_\tau^2} = 1 + \epsilon T_{11w} + \epsilon^2 T_{12w} + \dots + u_\tau \epsilon T_{21w} + \dots, \tag{5.20}$$

where T_{11} and T_{12} depend on σ, and T_{21} also depends on $\hat{y}/x$ and on $\ln u_\tau$; the subscript w refers to values at the wall.

As for the calculation of the pressure, it is desirable to combine the results in a composite solution which is correct for $x = O(1)$ and for small x, provided again that $\sigma - \sigma_a \gg \epsilon^{\frac{4}{3}}$, where σ_a is defined as before by $U_0(\sigma_a) = a^*$. It turns out that a simple modification of the intermediate solution suffices, with a factor $\kappa^{-1}(2\Pi + \ln 2)$ replaced by $-u_{01}(\frac{1}{2}x/B_0) + \sigma/u_\tau$. The first few terms in the expansion (5.20) at $\hat{y} = 0$ are

$$T_{11w} = \frac{1}{B_0}\left(\gamma M_0^2 - \frac{2U_0}{C_0 U_0'}\right), \tag{5.21}$$

$$T_{12w} = \frac{1}{B_0^2}\left\{\frac{U_0^2}{C_0^2 U_0'^2} - \frac{1+3\gamma}{2C_0 U_0'} M_0^2 U_0 + B_0\left(-1 + \frac{\gamma+1}{4}\frac{M_0^4}{B_0^2}\right) T_{11w}\right\}, \tag{5.22}$$

$$\begin{aligned} T_{21w} = {} & -\frac{1}{\kappa C_0}\left(\frac{\gamma M_0^2}{B_0} + T_{11w}\right) + (M_0^2 - 2)\left(1 + \frac{\gamma-1}{2} M_0^2\right)\frac{U_0' T_{11w}}{U_0 B_0^2} \\ & \times\left\{u_{01}\left(\frac{x}{2B_0}\right) - \frac{\sigma}{u_\tau}\right\} + \frac{2}{\kappa C_0 B_0}\left(1 + \frac{\gamma-1}{2} M_0^2 + \frac{U_0}{C_0 U_0'}\right) \\ & \times\left\{-2\Pi - \gamma_e + \ln\frac{2\kappa u_\tau B_0 U_0'}{U_0}\right\}, \end{aligned} \tag{5.23}$$

where γ_e is again the Euler constant. To see that the outer solution for τ_w is recovered as $\sigma \to 0$, it is necessary to expand T_{11w} as $\sigma \to 0$. It can be shown that the second term combines with other terms in a manner that yields the required form.

The composite solution for τ_w is compared in figure 4 with experimental data of Settles, Fitzpatrick & Bogdonoff (1979) for $\epsilon = 8°$, $M_\infty = 2.85$ and $u_\tau = 0.023$. The trend is predicted quite well, but the theoretical curve is about 20% too high. At values of x small enough that σ is close to the detachment value σ_d, the solution requires still further modification. Since $\tau_w = 1$ ahead of the corner, the value of τ_w must have a minimum. It appears that prediction of this minimum would require proper completion of the inviscid-flow solution very close to the corner, perhaps with the added effect of a very small separation bubble.

6. Concluding remarks

Close agreement of predicted and measured mean surface pressures has been demonstrated in particular cases, at $M_\infty \approx 4$ and $M_\infty \approx 5$ with $\epsilon \approx 15°$. The predicted values are based on analytical inviscid-flow solutions which describe small perturbations from a basic rotational wedge flow, with the undisturbed boundary layer characterized by a compressible-flow form of the velocity-defect law and the law of the wall. The solutions are obtained as the first terms in asymptotic expansions for small values of the non-dimensional friction velocity and the corner angle. For satisfactory accuracy it is found that a uniform flow is not adequate as a choice for the basic flow, but that a suitably improved representation can be achieved with the help of a hypersonic limit and appropriate intermediate limits. Fair agreement of the pressures is also obtained for a case with $M_\infty \approx 3$ and $\epsilon \approx 10°$.

The pressure calculations do not require any knowledge of the local changes in Reynolds stresses, and do not require introduction of an effective 'slip' Mach number at the wall. Partial solutions have also been derived at small distances from the corner

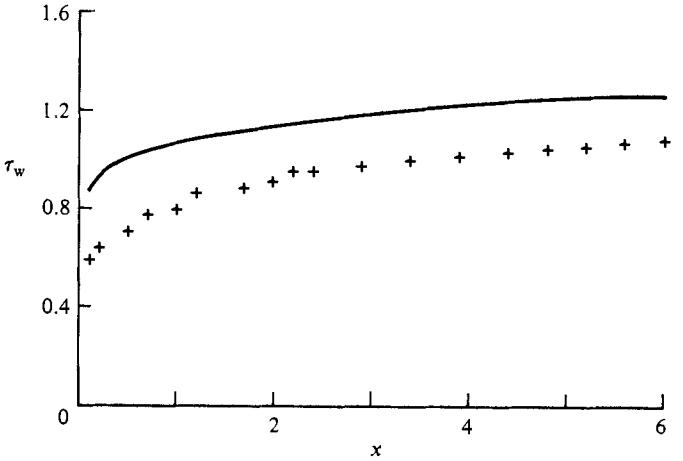

FIGURE 4. Wall shear stress for $M_\infty = 2.85$, $\epsilon = 8°$, $u_\tau = 0.02345$: ——, calculated from (5.20); +, experimental data (Settles *et al.* 1979).

such that the local Mach number is close to one. In the numerical examples considered, however, it appears that a very small region of reversed mean flow may have an appreciable effect for these lengthscales. The strong overshoot and subsequent gradual decrease in pressure which has been observed experimentally at $M_\infty \approx 2$ are still unexplained.

Calculation of changes in the wall shear stress requires matching a wall-layer solution with a solution to the boundary-layer momentum equation in a sublayer. A mixing-length model is found to give qualitative agreement with one set of experimental data. While this agreement seems encouraging, additional comparisons are needed, and better turbulence models should be considered, before a judgement can be made about the accuracy that might be expected for shear-stress distributions derived within the framework of the asymptotic theory.

This work was sponsored in part by the Office of Naval Research, Contract N00014-79-C-0285, NR 094-395; this support is gratefully acknowledged.

Appendix

When σ is close to σ_a, where $U_0(\sigma_a) = a^*$, different forms of expansion are needed. An expansion for u can be written in terms of variables σ^* and λ^*:

$$\sigma^* = \frac{\sigma - \sigma_a}{\epsilon^{\frac{2}{3}}}, \quad \lambda^* = \frac{x}{\epsilon^{\frac{1}{3}} y}, \tag{A 1}$$

$$u - a^* = \epsilon^{\frac{2}{3}} U_{11}^*(\sigma^*) + \ldots + u_\tau U_{21}^*(\sigma^*, \lambda^*) + \ldots . \tag{A 2}$$

The expansion for $v/\epsilon^{\frac{1}{3}}$ has the same form. Differential equations for U_{21}^* and V_{21}^* found from (2.5), (2.2) and (2.3) are

$$B_0^{*2} U_{21\lambda^*}^* + \lambda^* V_{21\lambda^*}^* = -\frac{1}{\kappa \lambda^*} B_0^{*2} U_{11\sigma^*}^*, \tag{A 3}$$

$$V_{21\lambda^*}^* + \lambda^* U_{21\lambda^*}^* = -\frac{1}{\kappa} M_\infty a^*, \tag{A 4}$$

where $B_0^{*2} = (\gamma+1)\,U_{11}^*/a^*$. The shock-polar equation gives

$$(M_\infty a^*\sigma^* - U_{11}^*)^2\,(M_\infty a^*\sigma^* + U_{11}^*) = \frac{2}{\gamma+1}a^{*3}, \tag{A 5}$$

$$\frac{4a^{*2}V_{21}^*}{(\gamma+1)\,(M_\infty a^*\sigma^* - U_{11}^*)} + (3U_{11}^* + M_\infty a^*\sigma^*)\,U_{21}^* = -\frac{1}{\kappa}M_\infty a^*(U_{11}^* + 3M_\infty a^*\sigma^*)\,(\ln\lambda^* + 2\Pi) \tag{A 6}$$

at $\lambda^* = \lambda_s^*$, where the equation for the shock-wave slope gives

$$\lambda_s^* = a^*/(M_\infty a^*\sigma^* - U_{11}^*).$$

The solution for U_{21}^* is

$$\kappa U_{21}^* = \frac{1}{2}\left(\frac{\mathrm{d}U_{11}^*}{\mathrm{d}\sigma^*} - M_\infty a^*\right)\ln\frac{\lambda^{*2} - B_0^{*2}}{\lambda_s^{*2} - B_0^{*2}} - \frac{\mathrm{d}U_{11}^*}{\mathrm{d}\sigma^*}\left(\ln\frac{\lambda^*}{B_0^*} + 2\Pi\right) + \frac{2a^{*2}\,|B_0^{*2}|^{\frac{1}{2}}\,(M_\infty a^* - \mathrm{d}U_{11}^*/\mathrm{d}\sigma^*)}{(\gamma+1)\,(U_{11}^* - M_\infty a^*\sigma^*)\,(3U_{11}^* + M_\infty a^*\sigma^*)}G(\sigma^*), \tag{A 7}$$

where
$$G(\sigma^*) = \ln\frac{\lambda_s^* - B_0^*}{\lambda_s^* + B_0^*} \quad \text{for} \quad B_0^{*2} > 0$$

and
$$G(\sigma^*) = 2\tan^{-1}\frac{|B_0^{*2}|^{\frac{1}{2}}}{\lambda_s^*} \quad \text{for} \quad B_0^{*2} < 0.$$

It is seen that $U_{11\sigma^*}^* \to \infty$ when $3U_{11}^* + M_\infty a^*\sigma^* \to 0$, i.e., when $\sigma^* \to \sigma_d^* = 3(\gamma+1)^{-\frac{1}{3}}2^{-\frac{4}{3}}/M_\infty$. Still another solution is needed when $\sigma^* - \sigma_d^* = O(\chi^{\frac{4}{3}})$, where $\chi = u_\tau/\epsilon^{\frac{2}{3}} \ll 1$. In terms of variables $\bar\sigma = (\sigma^* - \sigma_d^*)/\chi^{\frac{2}{3}}$ and λ^*, expansions for u and v have the form

$$u = a^* + \epsilon^{\frac{2}{3}}(\bar U_{11} + \chi^{\frac{1}{3}}\bar U_{21} + \chi^{\frac{2}{3}}\bar U_{31}) + \dots, \tag{A 8}$$

$$v = \epsilon(a^* + \chi^{\frac{2}{3}}\bar V_{31}) + \dots, \tag{A 9}$$

where $\bar U_{11} = -\frac{1}{3}M_\infty a^*\sigma_d^*$ and $\bar U_{21} = \bar U_{21}(\bar\sigma)$. The differential equations for $\bar U_{31}$ and $\bar V_{31}$ are

$$(\gamma+1)\,\bar U_{11}\,\bar U_{31\lambda^*} + \lambda^* a^*\,\bar V_{31\lambda^*} = -(\gamma+1)\frac{1}{\kappa\lambda^*}\,\bar U_{11}\,\bar U_{21}', \tag{A 10}$$

$$\bar V_{31\lambda^*} + \lambda^*\bar U_{31\lambda^*} = 0. \tag{A 11}$$

The shock-polar equation gives

$$2\frac{\bar V_{31}}{a^*} + \frac{3}{16}\frac{\bar U_{21}^2}{\bar U_{11}^2} - 3\frac{\bar\sigma}{\sigma_d^*} = 0. \tag{A 12}$$

The solution for $\bar V_3$ is proportional to $\bar U_{21}'$:

$$\bar V_3 = -\frac{1}{\kappa}2^{-\frac{2}{3}}(\gamma+1)^{\frac{1}{3}}\frac{\mathrm{d}\bar U_{21}}{\mathrm{d}\bar\sigma}\tan^{-1}\frac{2^{-\frac{2}{3}}(\gamma+1)^{\frac{1}{3}}}{\lambda^*}. \tag{A 13}$$

Substitution in the shock-polar equation (A 13), with $\lambda^* = 2^{-\frac{2}{3}}(\gamma+1)^{\frac{1}{3}}$ at the shock wave, leads to a Riccati equation for $\bar U_{21}$. The solution is

$$\bar U_{21} = -\tfrac{4}{9}a^* M_\infty\left(\frac{\sigma_d^*}{b}\right)^{\frac{1}{2}}\frac{\mathrm{Ai}'(b\bar\sigma)}{\mathrm{Ai}(b\bar\sigma)}, \tag{A 14}$$

where $b^{\frac{3}{2}} = 6\pi^{-1}\kappa(\sigma_d^*)^{-\frac{1}{2}}$ and Ai is the Airy function.

The solution (A 14) is bounded for $\bar{\sigma} > 0$, but Ai ($b\bar{\sigma}$ is oscillatory for $\bar{\sigma} < 0$, the first zero occurring at $\bar{\sigma} = \bar{\sigma}_0$, where $b\bar{\sigma}_0 \approx -2.34$. The term $\chi^{\frac{1}{3}}\bar{U}_{21}$ is no longer small in comparison with $\bar{U}_{11}$ when $\bar{\sigma} - \bar{\sigma}_0 = O(\chi^{\frac{1}{3}})$, i.e. when $\sigma - \sigma_d = O(u_\tau)$, where $\sigma_d = \sigma_a + \epsilon^{\frac{2}{3}}\sigma_d^* + \epsilon^{\frac{2}{3}} u_\tau^{\frac{1}{3}} \bar{\sigma}_0$. This condition is equivalent to the condition that a nonlinear differential equation be obtained in the first approximation. Then $U_0(\sigma_d)$ provides a three-term approximation to the upstream velocity u_u, defined by (2.15), at the location $y = y_d$ where shock-wave detachment occurs. In a limit with y/y_d and $\epsilon^{-\frac{1}{3}}x/y_d$ held fixed, the first approximation is described by the nonlinear transonic small-disturbance equations. The shock wave is detached, and as $y/y_d \to \infty$ the slope approaches that for an oblique shock wave which turns the flow through an angle ϵ at a Mach number $M_0(\sigma_d)$. The flow problem is easily formulated in the subsonic part of the hodograph plane, but, as noted in §4.2, may not be relevant for typical numerical values of the parameters.

REFERENCES

Adamson, T. C. 1976 The structure of shock wave–boundary layer interactions in transonic flow. In *Symposium Transsonicum II* (ed. K. Oswatitsch & D. Rues), pp. 244–251. Springer.

Adamson, T. C. & Feo, A. 1975 Interaction between a shock wave and a turbulent boundary layer in transonic flow. *SIAM J. Appl. Maths.* **29**, 121–145.

Adamson, T. C. & Liou, M. S. 1980 Interaction between a normal shock wave and a turbulent boundary layer at high transonic speeds. Part II: Wall shear stress. *Z. angew. Math. Phys.* **31**, 227–246; also *NASA CR* 3194.

Agrawal, S. 1983 Asymptotic theory of an unseparated supersonic turbulent boundary layer at a compression corner. Ph.D. thesis, University of Michigan, Ann Arbor.

Appels, C. & Richards, B. E. 1975 Incipient separation of a compressible turbulent boundary layer. *AGARD CP* 168, *Paper* 21.

Bush, W. B. 1971 On the Lagerstrom mathematical model for viscous flow at low Reynolds number. *SIAM J. Appl. Maths* **20**, 279–287.

Chu, B. T. 1952 On weak interaction of strong shock and Mach waves generated downstream of the shock. *J. Aero. Sci.* **19**, 433–446.

Dolling, D. S. & Murphy, M. T. 1983 Unsteadiness of the separation shock wave structure in a supersonic compression ramp flowfield. *AIAA J.* **21**, 1628–1634.

Elfstrom, G. M. 1972 Turbulent hypersonic flow at a wedge-compression corner. *J. Fluid Mech.* **53**, 113–127.

Guiraud, J. P. 1957 Écoulements hypersoniques infiniment voisins de l'écoulement sur un dièdre. *C.R. Acad. Sci. Paris* **244**, 2281–2284.

Maise, G. & McDonald, H. 1968 Mixing length and kinematic eddy viscosity in a compressible boundary layer. *AIAA J.* **6**, 73–80.

Melnik, R. E. 1981 Turbulent interactions on airfoils at transonic speeds – recent developments. *AGARD CP* 291, *Paper* 10.

Melnik, R. E. & Grossman, B. 1974 Analysis of the interaction of a weak normal shock wave with a turbulent boundary layer. *AIAA Paper* 74–598.

Messiter, A. F. 1980 Interaction between a normal shock wave and a turbulent boundary layer at high transonic speeds. Part I: Pressure distribution. *Z. angew. Math. Phys.* **31**, 204–226; also (with appendices) *NASA CR* 3194.

Rosen, R., Roshko, A. & Pavish, D. L. 1980 A two-layer calculation for the initial interaction region of an unseparated supersonic turbulent boundary layer with a ramp. *AIAA Paper* 80-0135.

Roshko, A. & Thomke, G. J. 1969 Supersonic turbulent boundary-layer interaction with a compression corner at very high Reynolds number. In *Proc. ARL Symp. on Viscous Interaction Phenomena in Supersonic and Hypersonic Flow*, pp. 109–138. University of Dayton Press, Dayton, Ohio.

ROSHKO, A. & THOMKE, G. J. 1976 Flare-induced separation lengths in supersonic turbulent boundary layers. *AIAA J.* **14**, 873–879.

SEARS, W. R. 1950 The linear-perturbation theory for rotational flow. *J. Maths & Phys.* **28**, 268–271.

SETTLES, G. S., FITZPATRICK, T. J. & BOGDONOFF, S. M. 1979 Detailed study of attached and separated compression corner flowfields in high Reynolds number supersonic flow. *AIAA J.* **17**, 579–585.

SYKES, R. I. 1980 An asymptotic theory of incompressible turbulent boundary-layer flow over a small hump. *J. Fluid Mech.* **101**, 647–670.

VAN DRIEST, E. R. 1951 Turbulent boundary layer in compressible fluids. *J. Aero. Sci.* **18**, 145–160.

VAN DYKE, M. D. 1954 A study of hypersonic small-disturbance theory. *NACA TN* 3173.

VAN DYKE, M. D. 1975 *Perturbation Methods in Fluid Mechanics.* Parabolic.